

## Review Article

# Injection molded high precision freeform optics for high volume applications

Lars Dick<sup>1,2,\*</sup>, Stefan Risse<sup>3</sup>  
and Andreas Tünnermann<sup>2,3</sup>

<sup>1</sup>JENOPTIK Optical Systems, JENOPTIK Polymer Systems GmbH, Am Sandberg 2, 07819 Triptis, Germany

<sup>2</sup>Friedrich-Schiller-University Jena, Abbe Center of Photonics, Institute of Applied Physics, Albert-Einstein-Str. 15, 07745 Jena, Germany

<sup>3</sup>Fraunhofer Institute for Applied Optics and Precision Engineering, Albert-Einstein-Str. 7, 07745 Jena, Germany

\*Corresponding author  
e-mail: lars.dick@jenoptik.com

Received December 20, 2011; accepted February 9, 2012

## Abstract

Injection molding offers a cost-efficient method for manufacturing high precision plastic optics for high-volume applications. Optical surfaces such as flats, spheres and also aspheres are meanwhile state-of-the-art in the field of plastic optics. The demand for surfaces without symmetric properties, commonly referred to as freeform surfaces, continues to rise. Currently, new mathematical approaches are under consideration which allow for new complex optical designs. Such novel optical designs strongly encourage development of new manufacturing methods. Specifically, new surface descriptions without an axis of symmetry, new ultra precision machining methods and non-symmetrical shrinkage compensation strategies have to be developed to produce freeform optical surfaces with high precision for high-volume applications. This paper will illustrate a deterministic and efficient way for the manufacturing of ultra precision injection molding tool inserts with sub-micron precision and show the manufacturing of replicated freeform surfaces with micrometer range shape accuracy at diameters up to 40 mm with a surface roughness of approximately 2 nm.

**Keywords:** freeform surface; injection molding; plastic optic; slow tool servo technology; ultra precision manufacturing.

## 1. Introduction

Modern optical systems applied to optical key markets such as mobile communication, healthcare, sensoric, security, lighting and also photovoltaics need to have more complex optical surfaces to achieve enhanced performance requirements

and/or reduced installation space [1–3]. One possibility to achieve these challenging goals is the application of freeform surfaces within the optical system. Products such as head-mounted displays, head-up displays, detector elements, varifocal glasses or also innovative LED illumination optics require freeform optics to guarantee an excellent function [4–7]. Especially by manufacturing imaging optics, the demands regarding a minimal deviation are very high. The complete process chain from the optical design up to the assembly of freeform optical systems is currently systematically analyzed in the research project ‘FREE’, funded by the German Federal Ministry for Education and Research [8].

In comparison to classical optical surfaces such as flats, spheres and aspheres, the axis of rotation at freeform surfaces is missing. In this case, the injection molding tool inserts cannot be manufactured using the traditional and common two-axis diamond turning technology. For a freeform surface, modern multiple axis ultra precision technologies in combination with monocrystalline diamond tools have to be used [9]. In the manufacturing of rotational symmetric surfaces with two-axis diamond turning at the mold with surface accuracies of peak to valley (p-v)  $< 0.5 \mu\text{m}$  (at diameters up to 40 mm) can be realized and considered state-of-the-art. This procedure cannot be applied to freeform surfaces generation. Here, complex and time-consuming manufacturing processes with more degrees of freedom have to be used. To push the accuracy into the range of p-v  $< 0.5 \mu\text{m}$ , new methods have to be developed.

This paper will explain the injection molding process chain, show a classification of freeform surfaces and define a typical freeform optic followed by some details about data handling between iteration loops. In addition, a deterministic way to realize freeform surfaces on a mold insert to achieve form accuracies of  $< 0.5 \mu\text{m}$  p-v will be discussed. Furthermore, plastic freeform optics are molded, where a common optimization of the deviation is done by the molding process parameters. Replicated freeform optical elements usually generate an irregular thickness over the surface, unlike a rotational symmetric lens where the thickness from the middle to the outer diameter is equal in every cross-section. Therefore, in most cases the main shrinkage in freeform optics will also be non-symmetrical, especially if the asymmetric content is significant. To compensate for such type of non-uniform shrinkage, a new process chain will be defined and demonstrated in this paper. As a result of this new process chain, a molded plastic freeform lens with accuracies of approximately  $2 \mu\text{m}$  over a diameter of 40 mm can be achieved, compared with approximately  $20 \mu\text{m}$  surface errors achieved by the current way which is state-of-the-art. Thus, the form deviation was successfully pushed from the typical range of illumination optics into the level of some imaging applications at molded plastic optics.

## 2. Process chain for manufacturing high precision freeform optics by injection molding

In general, the process chain for molding a freeform optical component is analog to molding rotational symmetric optical elements. Beyond the actual injection molding process, the material preparation as well as the following automation and quality assurance processes are common for this type of process (Figure 1).

With regard to the optical performance of plastic optics, properties of the raw material must be considered such as the molecular structure, the molecular conformation and impurities. Currently, the materials most commonly used for molding plastic optics are PMMA (polymethylmethacrylate), PC (polycarbonate), PS (polystyrol), COP (cyclo olefin polymer) and COC (cyclo olefin copolymer) [10]. In addition to molding plastic optics, also the molding of glass is possible where the process chain looks different to the injection molding process because of the other material properties of glass. Here, for example, higher process temperatures, longer cycle times and other mold materials have to be considered [11].

The basic elements within the process chain are the mold tool and the injection molding machine (Figure 2A,B). An injection molding tool as well as an injection molding machine are shown in general in the following pictures of which in practice many different designs and types exist [10, 12].

After material preparation and mounting the injection molding tool onto the injection molding machine, the molding process can be started. The following process steps have to be passed within one injection molding process, where after step 6 the cycle starts again with step 1 [10]:

1. cycle start, mold is open
2. mold closing
3. injection phase (cavity filling phase)
4. holding pressure phase (compression phase)
5. cooling phase, plasticizing process for next cycle
6. mold opening, part ejection

For high volume products often a multiple cavity tool can be used where more parts (e.g., 2, 4, 8, 16, 32, ...) can be molded within one cycle [10, 12].

After the cavity is packed (filled) with the plastic melt, the cooling process begins. As the lens is freezing and cools down to room temperature, whether the part is in the mold or has already been ejected, shrinkage and deformation will occur. The magnitude of this shrink effect is determined by the relationship between the specific volume ( $v$ ), temperature ( $T$ ) and pressure ( $p$ ) what can be seen in the  $p$  $v$  $T$  diagram for each material. The big challenge in molding freeform optical elements is the compensation of the systematic shrinkage of the molding resin on the optical lens surfaces. This compensation



**Figure 1** Process chain of injection molding of freeform optical elements [10].

needs to be incorporated into the manufacturing of the mold inserts. The accurate measurement of the mold inserts as well as the lens optical surfaces in 3D is required, and the compensation strategy for elimination of the shrinkage effect must be done in an efficient way.

## 3. Classification of freeform surfaces

Because there are different types of freeform surfaces, a classification is required where the freeform surface discussed in this paper can be characterized.

Freeform surfaces can be subdivided by different criteria. One can be the designation between imaging and illumination optics which dictate the needed accuracies of the optical surfaces. In general, imaging optics require much higher quality than illumination optics. Another classification is by geometric characteristics of the surface. An example of classification by the deviation of symmetry and the continuity is shown in Figure 3 [13].

The profile of the freeform surface has a direct influence to the required ultra precision manufacturing method of the mold, as well as to the measurement system.

This paper focuses on continuous freeforms with low frequent surface deviations of rotation symmetry. In this case, a modified turning method, referred to 'slow tool servo technology' is an optimal machine concept for ultra precision machining of the mold insert. For measurement and evaluation of such type of surfaces, tactile measurement methods can be used.

## 4. Exemplary freeform optic for process evaluation

For analyzing the whole process chain of injection molding freeform surfaces including novel correction strategies, an exemplary freeform surface has to be defined by a mathematic equation. Furthermore, the freeform optical surface has to be integrated into an optic volume element able for molding.

The main applications described in the introduction are continuous freeform surfaces with low frequent deviations. In searching for such a freeform surface an exemplary Zernike polynomial function was found. It can be calculated mathematically exactly by Eq. (1), which represents the sum of a non-rotational symmetric and a rotational symmetric part:

$$\begin{aligned}
 Z_{freeform}(x,y) &= Z_{nrs}(x,y) + Z_{rs}(x,y) \\
 &= z_{zernike}(4,4) \cdot \sqrt{10} \cdot \left( \frac{\sqrt{x^2+y^2}}{20} \right)^4 \cdot \cos \left( 4 \cdot \arctan \left( \frac{y}{x} \right) \right) \\
 &\quad + \frac{\frac{1}{R} \cdot (x^2+y^2)}{1 + \sqrt{1 - \left( \frac{1}{R} \right)^2 \cdot (x^2+y^2)}}
 \end{aligned} \tag{1}$$

Within the Cartesian coordinates ( $x$ ,  $y$ ,  $z$ ),  $z$  is the sag at a defined  $x$  and  $y$  position. The non-symmetrical term ( $Z_{nrs}$ )

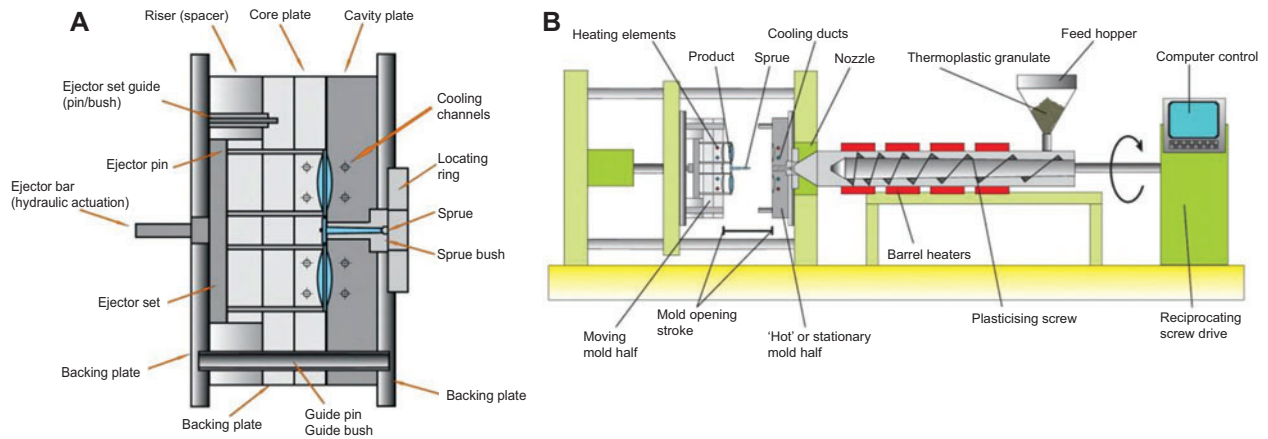


**Figure 2** (A) Typical elements of an injection mold [10]. (B) Typical elements of an injection molding machine [10].

is described by the  $z_{Zernike}^{(4,4)}$  term with 0.2, normalized to a radius of 20 mm. The  $z_{Zernike}^{(4,4)}$  term describes a so-called ‘Tetrafoil’ from the defined Zernike series. The rotational symmetric part ( $Z_{rs}$ ) is a convex sphere with a radius of  $R=100$  mm.

The deviation of the non-rotational symmetric part is 1.26 mm with a maximal slope of  $18.4^\circ$  at the clear aperture diameter of 40 mm. At the pitch circle in the outer area three spherical elements are positioned that provide an optional referencing of the freeform surface in the measurement or the optical system. The designed optical element has this one freeform surface. The second optical surface is a flat.

The designed freeform surface has to be implemented into an optical volume element, which is dedicated for the molding process. For this freeform lens, the gate position can be seen and a bevel at the outer diameter was added for manufacturability (see Figure 4A,B). The outer diameter of the part is 70 mm and the center thickness is 5.5 mm. The material for the lens is PMMA 7N.

## 5. Data handling for high accuracies at the mold as well as at the molded freeform lens

Producing the optical freeform surface for the injection mold, ultra precision machines have to be programmed with exact numerical data for the complete surface. In general, non-rotational symmetric surfaces can be nominally described by Splines, NURBS (Non-Uniform Rotational B-splines), B-splines, Zernike polynomials,  $xy$  polynomials/extended polynomials, as well as point clouds. For example, typical transfer formats IGES, STEP and point clouds [7, 14, 15].

For the first cut of the defined optical freeform surface utilizing the slow tool servo machining process, the tool path was generated by an Zernike mathematical description loaded directly into an ultra precision CAM (computer-aided manufacturing) software. In this case, the commercial software DiffSys (Western Isle Ltd, Denbigh, North Wales, GB, Version 3.82) was used allowing for additional the tool radius compensation of the diamond tool. The designed surface in

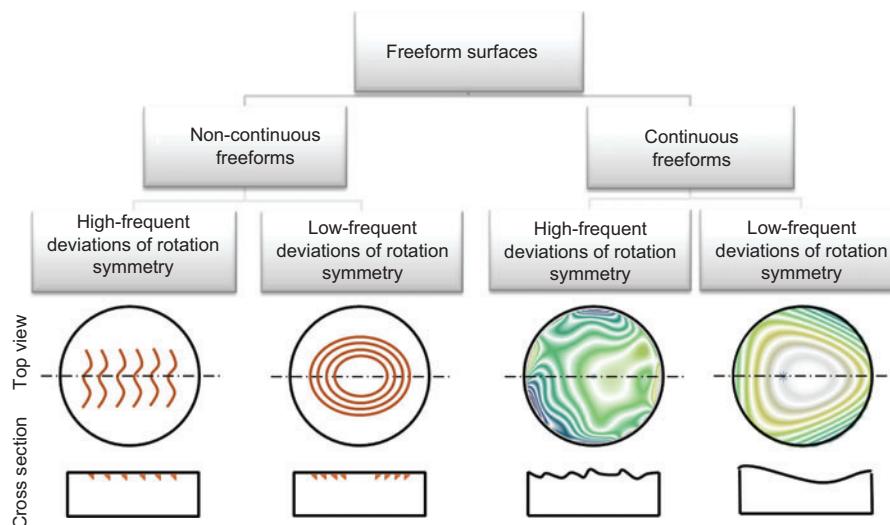


**Figure 3** Classification of freeform optical surfaces [13].

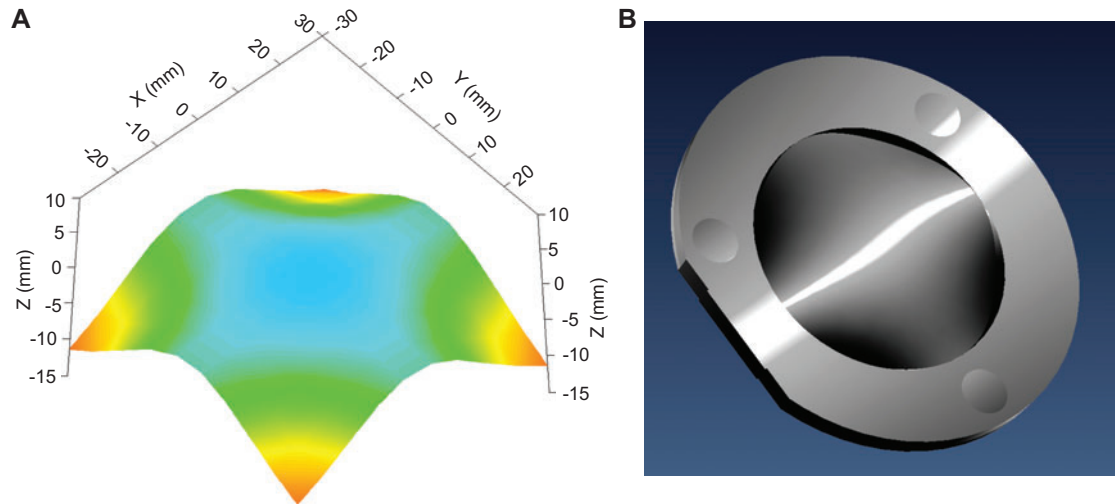


**Figure 4** (A) Designed freeform surface for developing the process chain. (B) Designed optical element for injection molding in 3D CAD.

CAM (Figure 5A) and the resulting  $z$  dynamic can be found in Figure 5B for different  $X$  positions at the defined surface. The maximum curvature in cutting direction can be seen at the outer diameter of 40 mm with  $0.024 \text{ mm}^{-1}$ .

For a correction loop at the processed tool insert as well as for the shrinkage compensation of the molded part, a 3D measurement has to be done to generate data regarding the surface deviation to the nominal design surface. The measurement of the Zernike surface was done by an ultra accuracy 3D profilometer (UA3P-5) with an accuracy of  $<50 \text{ nm}$  at this type of surface [16]. Because, in fact, most measurement software systems cannot evaluate freeform surfaces, tactile measurement systems typically will export the points cloud from the middle of the stylus and a normal vector, and not the real measured surface data or the deviation.

To identify the real surface points, a tool tip correction has to be done with the given normal vectors and the tip radius of used stylus. A further step is the calculation of the shape deviation of the freeform surface, because positioning errors

of the mold/molded freeform surface regarding the coordinate system of the measuring system are given. Hereby, especially two strategies are discussed to address this.

The first is a mathematical iteration where position errors are minimized. This is achieved by shifting and tilting the mathematical freeform description up to 6 degrees of freedom to the measured points cloud. For the Zernike surface, this is explained in more detail in the literature [17].

A second way is to calculate the form deviation regarding some well-defined reference points explained in [18] and [19], whereby some spherical elements, for example, can be a basis to the freeform surface.

The 'best fit' strategy is explored in this paper, but the second approach is also possible within the given process chain as the evaluated deviation can be considered in the same way.

If the mathematical description of the freeform surface is known in addition to the form deviation (of the mold insert itself and/or the molded part), a new freeform surface can be calculated where a Cartesian points cloud ( $xyz$ ) will define the

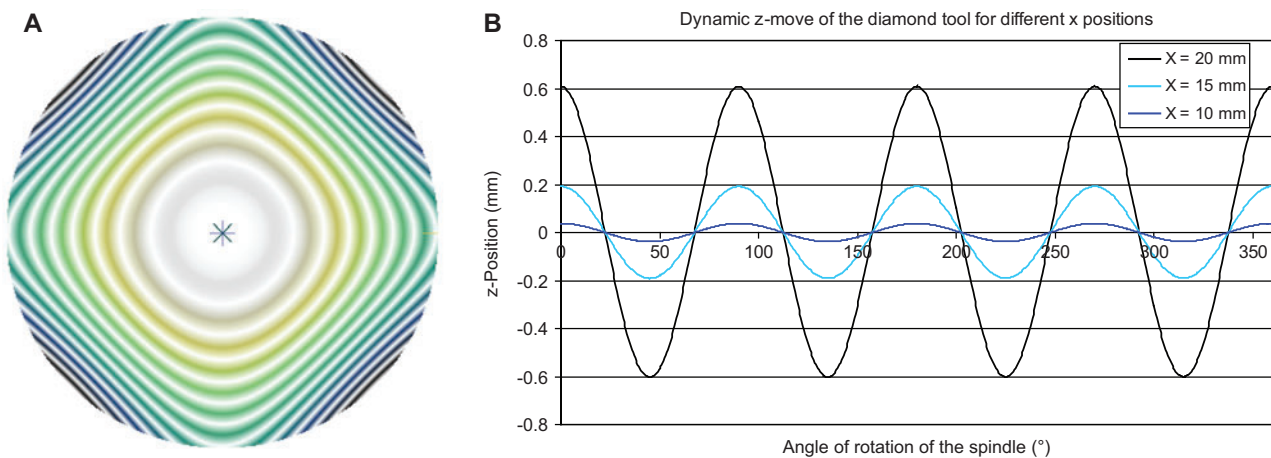


**Figure 5** (A) Programmed freeform surface in the CAM software. (B) Dynamic movement of the  $z$ -axis at different  $x$ -positions by manufacturing of the defined Zernike surface.

transfer format to the CAM system. A new tool path for an iteration loop has to be generated in polar coordinates ( $cxz$ ) for slow tool servo technology where a spiral is described. The CAM software will then have to interpolate between the imported points raster where the data quality is influenced. To prove the interpolation accuracy in the CAM software DiffSys, some experiments were done at the defined Zernike surface itself. Different raster sizes were imported and the tool path was calculated and compared with the exact mathematical description of the freeform surface for different  $x$  positions/curvatures. In DiffSys, two interpolation strategies can be used, linear interpolation or spline interpolation. The different results can be seen in Figure 6.

In general, one can see that the interpolation accuracy depends on the imported raster size and the interpolation algorithm where a smaller raster size and spline interpolation each has a positive influence on the interpolation accuracy.

The spline interpolation generates a sag error of  $<2$  nm across the entire surface by an imported raster size of  $0.1 \times 0.1$  mm compared to the linear interpolation that creates an error from 25 nm at  $R=5$  mm up to 43 nm at the outer diameter. The generated sag error using big raster sizes of  $1 \times 1$  mm and linear interpolation shows a multiple error from  $2.51 \mu\text{m}$  at  $R=5$  mm to  $3.34 \mu\text{m}$  at the highest curvature at the outer diameter, where the analyzed spline interpolation present errors of 16–80 nm.

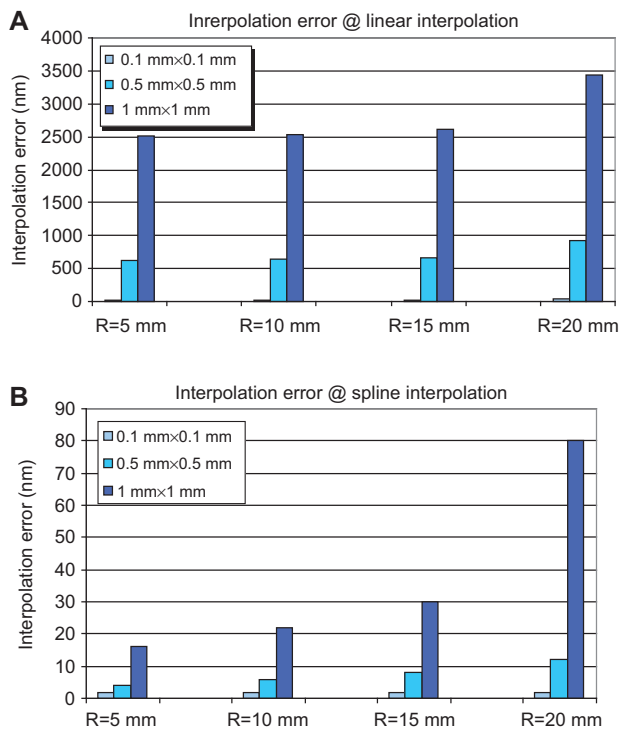


**Figure 6** (A) Interpolation errors of the CAM software by calculating a spiral tool path into a Cartesian point raster analyzed for linear interpolation. (B) Interpolation errors of the CAM software by calculating a spiral tool path into a Cartesian point raster analyzed for spline interpolation.

A review of the interpolation errors at small raster sizes and spline interpolation, the CAM system DiffSys 3.82 provides very accurate data with minimal loss of precision. This process can be used for iteration loops on homogeneous freeform surfaces with aimed accuracies with p-v values of  $<500$  nm.

## 6. Ultra precision manufacturing, error influences and error correction of the freeform optical surface at the mold

For manufacturing of the freeform optical mold, ultra precision machining methods utilizing a monocrystalline diamond tool as explained in [9] and [20] are preferred methods for an efficient machining. The surface explained above was designed for the slow tool servo technology. This process is qualified for generating smooth freeform surfaces where the two-axis diamond turning machine is modified with a CNC controlled rotation axis ( $c$ ) in addition to the two-linear axis ( $x$  and  $z$ ). The machine concept and typical frequency characteristics are shown in Figure 7. In addition, frequencies for fast tool servo systems can be seen.

The rotational symmetric deviation can be generated by two-linear axes where the non-rotational symmetric deviation of the freeform surface is generated by the dynamic diamond tool motion in the  $z$  direction (optical axis). The  $z$ -move for some  $x$  positions was shown in Figure 5B. Looking at the diagram in Figure 7B, the values have to be calculated for the defined Zernike surface. Manufacturing the defined Zernike surface with 15 rpm, a tool drive frequency  $F_d$  of 2 Hz can be calculated. With a drive amplitude of 0.63 mm at the outer diameter, the parameters for slow tool servo manufacturing can be easily obtained.

The accuracies achieved by diamond machining of freeform surfaces with a slow tool servo technology are influenced by some systematic errors such as tool decentration [22], axis position errors, radius error of the diamond tool and the measuring errors of them. In addition to the systematic errors noted, random errors such as temperature or pressure drifts will also affect the achievable accuracies during this time-consuming slow tool servo process and between iteration loops. For reference, the manufacturing time (finishing) for this defined Zernike surface was approximately 2 h, the time within one iteration loop can be as much as some days.

The primary systematic errors can be checked and evaluated as follows.

(i) The tool can be decentered in the vertical ( $x$ ) and the horizontal axis ( $y$ ). Setting the tool in the  $y$ -axis, an artifact at the turning center occurs. It is a cylinder if the diamond is below the center and a cone if the diamond is above the center. By measuring the diameter of the artifact, the tool height can be corrected very accurate and efficiently.

The horizontal offset in  $x$  can be seen for rotational symmetric surfaces with the help of the measurement result (character of the form deviation) best. For this type of surface, compensation strategies depending on the character of the

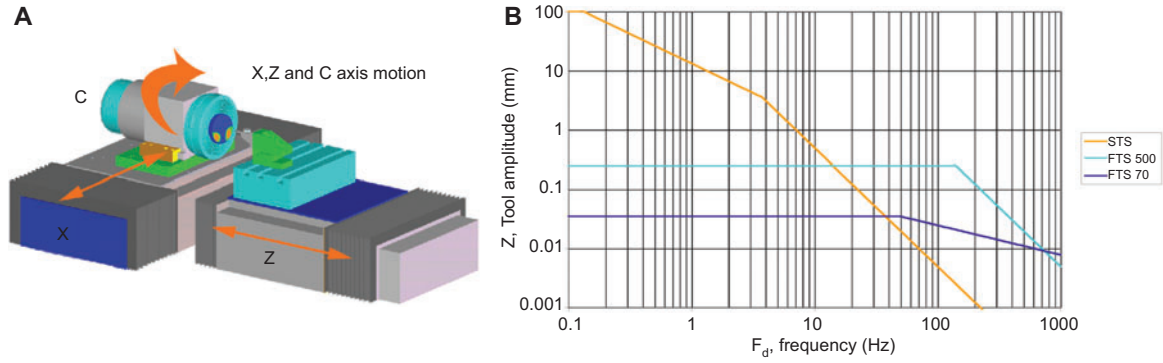


**Figure 7** (A) Machine concept and axes definition for slow tool servo technology [21]. (B) Surface frequency in connection with the doable surface amplitudes for slow tool servo technology as well as different fast tool servo systems [21].

form deviation and the concave or convex shape are state-of-the-art.

On freeform surfaces it cannot be seen so easily. For the defined Zernike surface on the mold insert (mirror image of the lens surface) different cases were simulated. Figure 8 shows the simulated deviation with a decenter in  $x$  of  $-5 \mu\text{m}$ . The resulted form deviation was  $1.25 \mu\text{m}$  p-v in the clear aperture diameter of 40 mm. Two scenarios were simulated, the left picture for turning the surface from  $x-$  to the center and the right part in the picture for turning from  $x+$  to the center. The deviation error for the full surface in each case has to be mirrored because the defined Zernike surface has a symmetry around both the  $x$ -axis and  $y$ -axis.

(ii) Position errors of the CNC controlled axis can be checked online at the machine and are shown in Figures

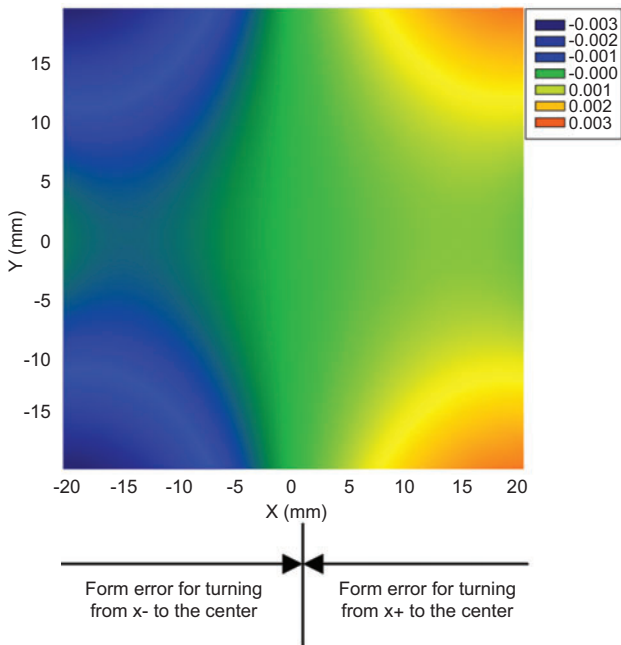


**Figure 8** Simulated deviation error caused by a decentration of the diamond tool vertically with an error of  $-5 \mu\text{m}$  in the  $x$ -axis.

9A–C for all CNC controlled machine axis at the high dynamic section at the outer diameter. The main error can be seen at the dynamic  $z$ -axis. In  $z$  the main dynamic section is approximately  $0.4 \mu\text{m}$  p-v, in  $x$  the following error is much more lower because there is a steady move of  $5 \mu\text{m}$  per revolution in  $x+$ . The  $z$ -error looks like the tool path itself in principle, which can be caused by the highest following error where the tool path has to be reversed at each movement. The rotational  $c$ -axis error has a minimal value of approximately  $0.0005^\circ$ .

(iii) The CAM software needs to know an actual radius of the diamond tip for calculating real positions for the machine axis. One problem regarding the diamond radius is the ideal measurement of it. Certainly, a high precision measurement can be done but a residual error is given. In addition, a radius error (waviness) of a monocrystalline diamond tool currently is typically  $<0.25 \mu\text{m}$ , an optimum  $<0.05 \mu\text{m}$  can be achieved [23]. This error generates a deviation at the manufactured surface depending on the curvature of the surface or what area of the diamond tip is used. In the experiments dealing with the defined Zernike surface a tool radius of 1.071 mm with a waviness of  $<50 \text{ nm}$  was used.

Next, random errors are given. For this, temperature gradients in the machine environment and pressure gradients (at the machine) have to be controlled very precisely [10]. A typical value for the temperature tolerance in the environment of ultra precision technology is  $<0.5^\circ\text{C}$ .

Understanding these main error influences, the defined Zernike surface was manufactured at the mold best possible according to the common procedure. The tool insert is a hardened steel substrate added with a special nickel phosphorous plating with a phosphorous content of  $>10\%$  for an efficient diamond machining process, where a roughness  $R_a < 5 \text{ nm}$  can be achieved [10]. The machined mold insert was measured at the high accuracy profilometer Panasonic UA3P-5. The measurement accuracy for this type of freeform surface (size, slopes) is  $<50 \text{ nm}$  [16]. The measured surface data were subsequently evaluated as explained above in Section 5. A surface accuracy with  $2.27 \mu\text{m}$  p-v and  $0.375 \mu\text{m}$  rms (root mean square) was measured at a clear aperture diameter of 40 mm (Figure 10A,B). Looking at the deviation surface before

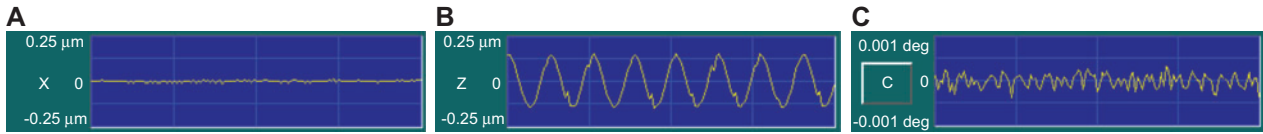


**Figure 9** (A) Position error of the linear axis  $x$ . (B) Position error of the linear axis  $z$ . (C) Position error of the axis of rotation  $c$ .

the correction loop, a picture like the simulated diamond tool error in Figure 8 can be seen for turning from  $x$ - to the center with a negative  $x$ -shift error.

To achieve a much higher precision at the mold freeform surface, a special iteration loop was developed. Fitting the deviation surface by a Fourier equation (Figure 10C) with a coefficient of determination  $r^2=0.9969$  to the measured data, the deviation surface can be superimposed to the Zernike surfaces where a new freeform surface can be calculated in a very high numerical precision. The even Fourier function additionally has an effect of smoothing the measurement data. After generating a new tool path in the CAM system, the freeform mold was generated where all the other technological process parameters have to be strongly the same as the first machining.

After one iteration loop, the form deviation was minimized from 2.27 μm p-v (0.375 μm rms) to 0.24 μm p-v (33.1 nm rms), which is nearly one order of magnitude. Looking at the form deviation after the correction loop (Figure 10E,F) compared with the residuals of the fit (Figure 10D), some similarities can be seen. The surface error after the iteration loop looks like the mathematical error smoothed. The reason can be found in the local accuracy of the fit. The fit covers the local errors of the surface but not as good as the global deviation. The local jumps can occur by the following errors of the  $z$ -axis because the artifacts can be seen every 45° systematically and the following errors can be seen in Figure 9B. Because these errors are not described exactly by the mathematical Fourier function, the systematic error by machining will be

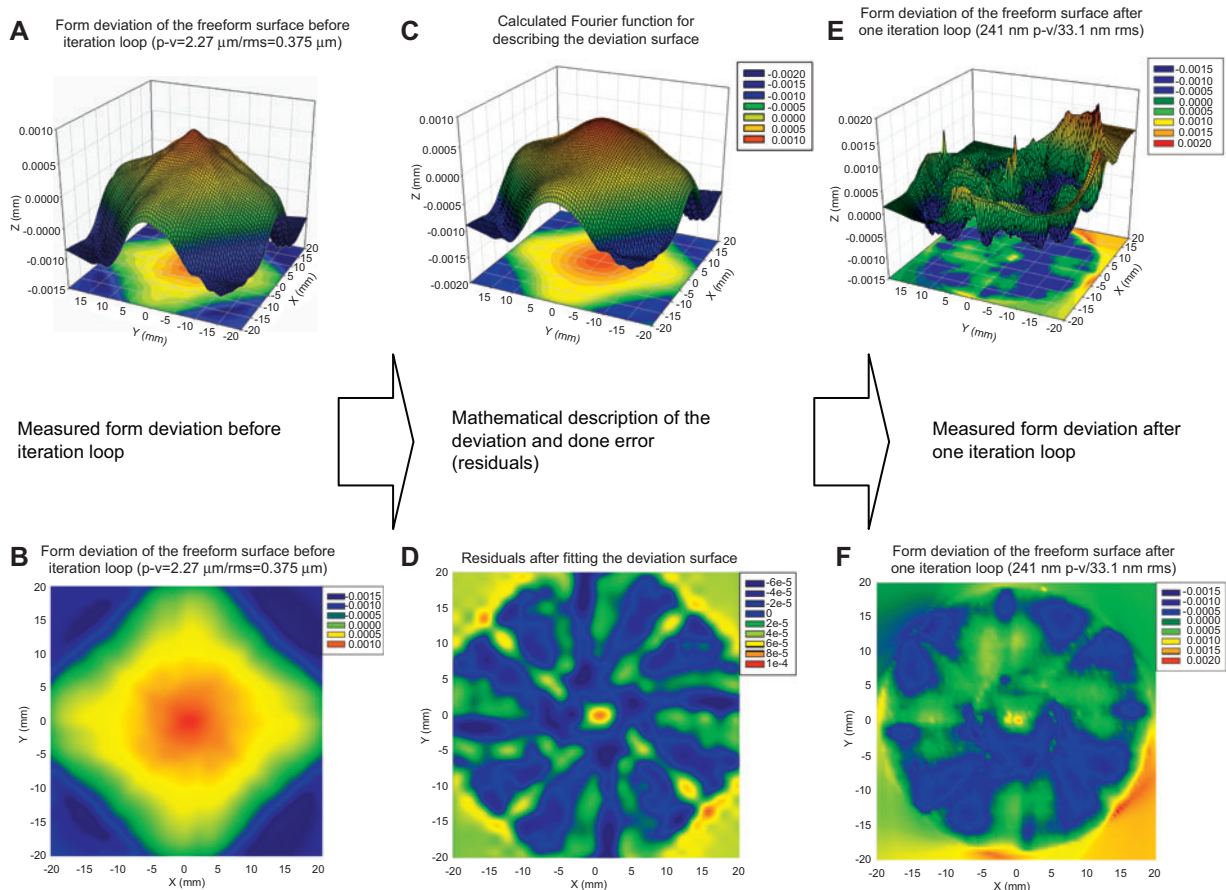


**Figure 10** Details of the iteration loop for the manufacturing of a high precision freeform surface on the mold. (A) Surface deviation before iteration loop, 3D view. (B) Surface deviation before iteration loop, top view. (C) Fitted Fourier function as error description of the surface deviation. (D) Error between fitted deviation and found mathematical description. (E) Surface deviation after one iteration loop, 3D view. (F) Surface deviation after one iteration loop, top view.

done again. As random errors affect process stability, the whole residuals from the surface deviation before correction loop cannot be seen. It is possible that a second iteration loop could make sense where a new deviation surface can be calculated.

## 7. Injection molding of high precision freeform surfaces with use of the developed iteration loop

A main element for the injection molding process is the injection mold as shown in Section 2. For practical experiments, the cavity as well as the complete injection mold was designed in 3D CAD software and manufactured. The classical configuration with the so-called nozzle and ejector side can be seen in the 3D CAD model (Figure 11A) as well as the manufactured tool (Figure 11B). The optical tool inserts were realized with slow tool servo technology (freeform insert, see Figure 11C) and two-axis diamond turning (plane optical insert). The non-optical elements were produced with classical tool shop methods such as milling, turning, grinding and electro discharge machining (sink and wire).

According to [24], the quality of molded parts is a result of a complex combination of the used material (according their  $pVT$  characteristics), the part and mold design as well as the process conditions. The resulting shrinkage is one of the several important factors affecting the quality of the molded part. Process parameters such as packaging pressure, dwell pressure, dwell pressure time, melt temperature and tooling temperature as well as cooling time have an influence, shown in [25]. The most significant influence parameter can be found in the packaging pressure [26, 27].

For the compensation of mechanical dimensions, a shrinkage rate of 0.2–1% (depending on the used plastic material) in all directions in space can be considered before manufacturing the mold. This was done in the CAD design for the defined Zernike freeform volume element with a value of 0.5% for PMMA. Because of non-linear shrinkage effects depending on the unique component geometry and molding process parameters, this standard process is not good enough for the optical surface. Also, FEM simulation tools actually cannot give a 1:1 forecast for the expected surface deviation. Thus, typically for the first molding process of optical

components, the nominal optical surface is manufactured [28]. In the case of the Zernike freeform, the optical surfaces were produced with the nominal optical description where the optical surface data of the lens have to be mirrored for the surface at the mold. The shrinkage can be influenced by design parameters, the gate and runner design, as well as process parameters such as dwell pressure, dwell pressure time, mold temperature cooling time, as well as tool concepts (e.g., temperature control versions) and using further replication techniques such as injection embossing [10]. Thus, in general, by injection molding high precision optics, a high dwell pressure and a long dwell pressure time is used to compensate the shrinkage. This can be done as long as the gate is molten so that the pressure can be active at the optical surface in the cavity. For rotational symmetric surfaces, often easily the most symmetric shrinkage can be compensated with a calculated symmetric geometry at the tool insert. Thus, for molding a spherical surface, an aspherical tool insert may be manufactured for molding the sphere in a high precision [12]. These machining methods, measurement and compensation methods in 2D are state-of-the-art. The compensation of non-linear deviation effects, especially in molding optical freeform surfaces is much more complex owing to the 3D measuring, data handling and machining methods.

For molding the defined Zernike freeform optical volume element, the finished injection mold was mounted on the injection molding machine where first processes were generated. First process parameters were defined with the help of the material data (PMMA) and known values for such type of geometries (thickness, size). These first process parameters resulted in a complete filled part in high quality where typical specifications for high precision plastic optics (bubbles, inclusions, thermal damages, flow marks could) were reached (see Figure 12).

Measuring the freeform surface analog with the tactile profilometer (as explained for the measurement at the tool insert), a deviation of approximately  $60\ \mu\text{m}$  p-v and  $16\ \mu\text{m}$  rms was analyzed (Figure 13A). This is a typical value for the deformation of a plastic lens in PMMA at this size and general geometry. A typical sink in the middle of the part at the thickest area of the lens can be seen. The random process variation of this generated freeform surface with this process was  $4.3\ \mu\text{m}$  p-v. Hence, this first process is not good enough for a compensation of the shrinkage

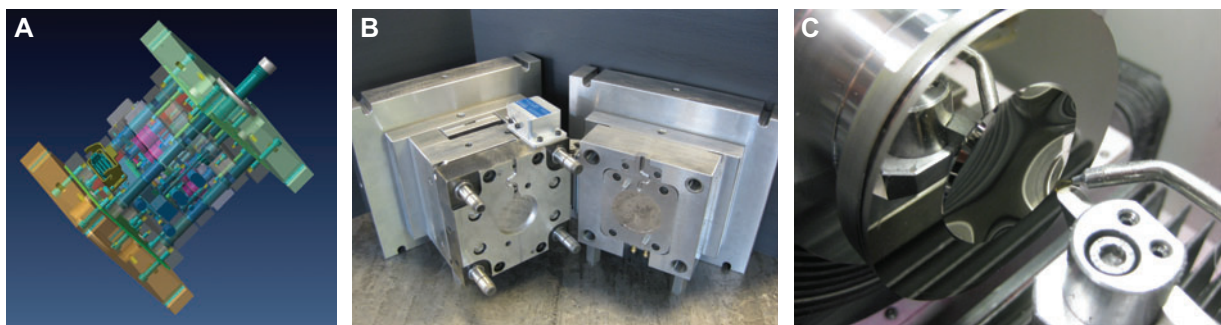


**Figure 11** (A) 3D CAD design of the mold tool. (B) Manufactured mold tool. (C) Freeform tool insert positioned at the vacuum chuck on the ultra precision machine and diamond tool.





**Figure 12** Molded freeform optical element with defined Zernike surface including gate.

by using the mold modification, especially owing to the process instability. To optimize this, other process versions were done. As a result, a better version was found with a process random error of  $1.38\ \mu\text{m}$  p-v or with a p-v value of approximately  $18\ \mu\text{m}$  and  $4\ \mu\text{m}$  rms. The first as well as the optimized molding parameters can be seen in Table 1. The deviation after process optimization looks asymmetric similar to the Zernike function itself in principal. Some exemplary measurements can be seen in Figure 13A,B. In addition, the birefringence was also measured with approximately  $150\ \text{nm}$  optical retardation within the freeform surface at the optimized process version regarding the surface deviation.

By the given process optimization the p-v values can be influenced very well but limitations are given. In addition, for an economical mass production a minimal p-v value and fast process cycles are often in conflict. To multiply the precision of the defined freeform surface, further process steps are required. In this regard, the measurement of the surface deviation at the molded part has to be described by a mathematical function. Following a new freeform surface for the mold can be calculated where the deviation of the molded freeform surface has to be superimposed to the Zernike sag itself at the tool insert. The new calculated surface comprises all the information which controls the systematic shrinkage effect

of the molding process. Before calculating the new surface for the tool insert, a transformation of the measured deviation surface has to be done, where the measurement has to be mirrored at the y-axis.

Transferring the points cloud with a raster size of  $0.1 \times 0.1\ \text{mm}$  to the CAM system as described in Section 5, the mold can be processed with the modified tool path. Reference elements for the angle and the xy-position for a high precision positioning of the mold are essential.

Molding the defined Zernike freeform optic again with the same molding process parameters but the modified tool insert, the molded freeform lenses were measured. A form deviation of approximately  $2\ \mu\text{m}$  p-v and  $0.28\ \mu\text{m}$  rms was reached by one iteration cycle, which is more than one order of magnitude more. One measurement with  $1.57\ \mu\text{m}$  p-v and  $0.253\ \mu\text{m}$  rms can be seen in Figure 14E,F. The p-v value occurs at the outer area, the middle area is very even. For example, at a diameter of  $22\ \text{mm}$ , a p-v value of  $<0.5\ \mu\text{m}$  was reproducibly reached.

Comparing this surface accuracy of the molded part with the deviation of a diamond turned surface without iteration loop, a better surface accuracy was reached by injection molding. Now, the process scattering with approximately  $1.3\ \mu\text{m}$  is the main problem for a second directed iteration loop where a systematic error surface is demanded. Random process variations cannot be corrected by this method.

The residuals shown in Figure 14D have a similarity with the residuals of the tool insert in Figure 10D, as well as the manufacturing result of a tool insert in Figure 10F. Thus, the high frequency errors were replicated by the molding process.

Problems within the process chain can be thermal drifts or other changing environmental conditions at the ultra precision machine, as well as the injection molding machine between the first and the second machining of the mold. Periods of some days have to be considered. To check the influence of the random variations at the ultra precision machine, the Zernike design surface should be manufactured and measured before the new calculated surface is processed. Thus, two conditions are given where the difference

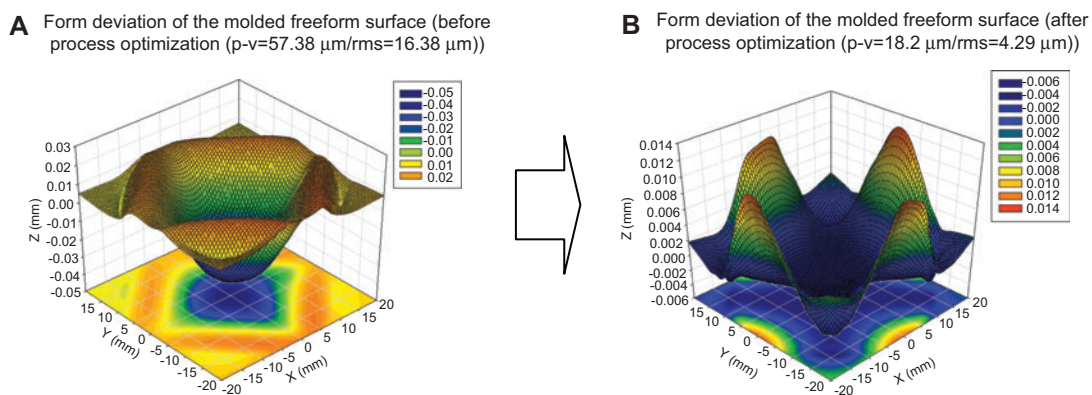


**Figure 13** (A) Form deviation of the molded freeform surface before process optimization, 3D view. (B) Form deviation of the molded freeform surface after process optimization, 3D view.

**Table 1** Start values (left) and optimized molding parameters (right).

Melt temperature	240°C	240°C
Packaging pressure	1500 bar	1500 bar
Dwell pressure	800 bar	1000 bar
Dwell pressure time	10 s	30 s
Tool temperature	100°C	90°C
Cooling time	120 s	180 s

between the two situations can also be calculated within the tool path.

The given algorithm of course can be used for the compensation of the non-linear shrinkage on surfaces with symmetry such as flats, spheres and aspheres. In [29], the non-linear shape deviation of a plane optical surface at a molded prism was successfully minimized from 12.6  $\mu\text{m}$  to approximately 2.72  $\mu\text{m}$  p-v.

## 8. Examinations of surface roughness

In addition to the form accuracy of optical surfaces, the micro roughness is a main quality factor. To influence the roughness

within the turning process, the parameters shown in the equation of Brammertz [30] can be modified. Thus, the diamond tool tip radius ( $r_\epsilon$ ) and the feedrate per revolution ( $f$ ) have a main influence to the roughness ( $R_{th}$ ), where a big tool tip radius and a small feedrate per revolution have a positive influence:

$$R_{th} = r_\epsilon \sqrt{r_\epsilon^2 - \frac{f^2}{4}} \approx \frac{f^2}{8r_\epsilon} \quad (2)$$

For the defined Zernike surface a feedrate of 5  $\mu\text{m}$  per revolution was used where a theoretical roughness of 2.9 nm should be achieved in theory. Certainly, other factors such as basic material, cutting parameters and vibrations also influence the roughness [28].

To check the roughness at the defined Zernike freeform surface after diamond processing and injection molding, some measurements at a white light interferometer were done. The following exemplary measurements were done at the highest asymmetric area at the outer diameter of the Zernike freeform surface. As a result, a roughness of 2.40 nm in  $R_a$  at the diamond turned mold was measured in a field of 1.4 mm $\times$ 1 mm. No additional polishing step was done after diamond

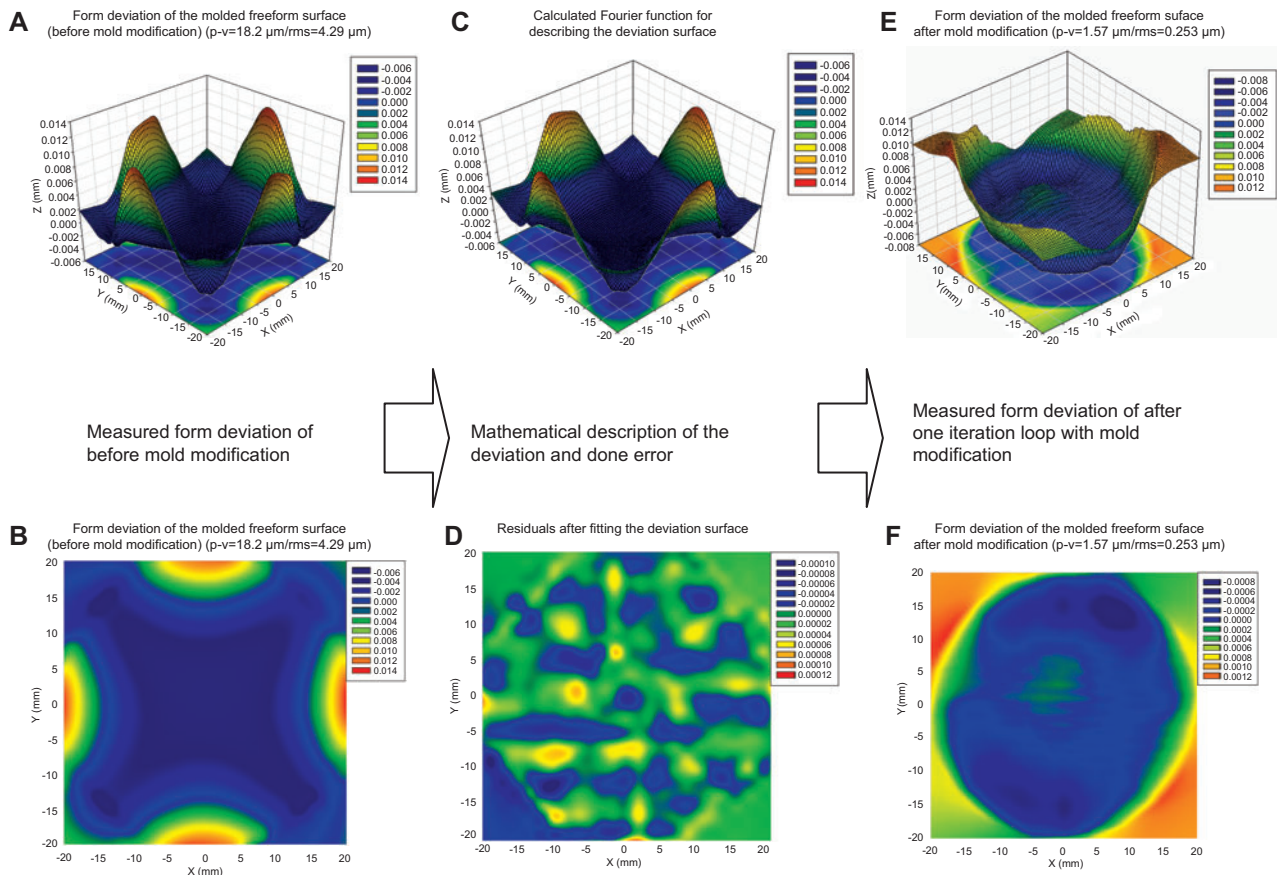


**Figure 14** Details of the iteration loop for the manufacturing of a high precision molded freeform surface. (A) Form deviation before iteration loop, 3D view. (B) Form deviation before iteration loop, top view. (C) Fitted Fourier function as error description of the deviation. (D) Error between fitted deviation and found mathematical description. (E) Form deviation after one iteration loop, 3D view. (F) Form deviation after one iteration loop, top view.

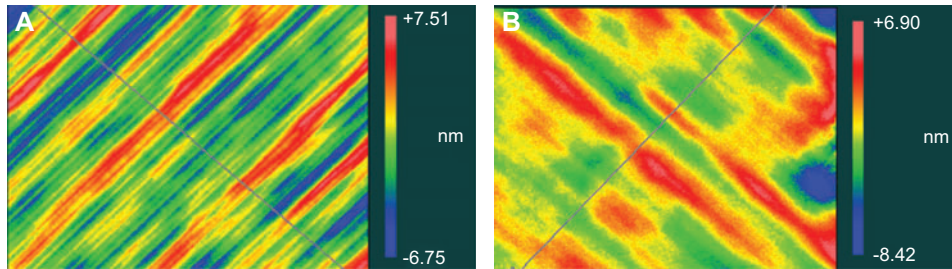


**Figure 15** Comparison of roughness at the mold and the molded freeform optical surface. (A) Measured roughness at the mold with 2.4 nm  $R_a$ . (B) Measured roughness at the molded freeform surface with 1.99 nm  $R_a$ .

machining the mold, which is possible in addition to the given process. Interesting is the analysis of the molded lens at the same location. Here, the roughness is a little bit smoothed with a  $R_a$  of 1.99 nm where the picture looks smoothed. A reason for this could be that the roughness peaks at the mold cannot be filled by the molding process completely.

## 9. Conclusions

Freeform optical surfaces are currently a big challenge in the field of modern optic applications. For a high-volume market, injection molding is a manufacturing method of choice for cost-efficient and high precision freeform optics. To increase the accuracy of the freeform surface at the molded lens compared to the state-of-the-art, the accuracy at the mold has to be increased and an efficient 3D shrinkage compensation strategy is necessary.

This paper discusses a process chain for producing ultra precision freeform optical surfaces at the mold and at the molded lens. With each additional process step, the accuracy was increased by one order of magnitude. For this, ultra precision machining, high precision measurement and an injection molding process of freeform surfaces was combined in an efficient way. An essential factor for success is the data handling between the iteration loops, which was also shown in detail.

With the novel process chain, freeformed shape deviations have been successfully minimized to 0.24  $\mu\text{m}$  p-v at the mold and to approximately 2  $\mu\text{m}$  at the molded freeform surface at a diameter of 40 mm. The reached manufacturing accuracies prove that a deterministic process chain was found, which allows the manufacturing of novel high precision freeform optics for high volume applications. The form deviation was successfully pushed from the typical range of illumination optics into the level of some imaging applications such as head up- or head-mounted displays in high volume.

Future activities will concentrate on improvement of process stability of the injection molding and further iteration loops.

## Acknowledgments

The presented research work is funded within the FREE project by the Federal Ministry for Education and Research (Grant No. JENOPTIK

Polymer Systems GmbH: 13N10826, Grant No. Fraunhofer IOF 13N10827). The authors acknowledge this funding for efficient research.

## References

- [1] D. Michaelis, P. Schreiber and A. Bräuer. Optics Lett. 36, 918–920 (2011).
- [2] S. Zwick, P. Kühmstedt and G. Notni. in ‘Phase-shifting fringe projection system using freeform optics’, Proc. SPIE, 8169–33 (2011).
- [3] L. Li and A. Y. Yi, J. Opt. Soc. Am. 27, 2613–2620 (2010).
- [4] H. Ries and J. Muschaweck, J. Opt. Soc. Am. 19, 590–595 (2002).
- [5] S. Riehemann, M. Palme, R. Steinkopf, P. Munzert, G. Notni, et al., in ‘Monolithisches optisches Freiformelement für eine IR-Detektorzeile’ (DGAO Tagung Ilmenau, 2011).
- [6] R. Eberhardt, in ‘Freiformoptik – Die Herausforderung für zukünftige optische Systeme’, LASER + PHOTONIK, 3/2010 (2010) pp. 38–39.
- [7] P. Ott, in ‘Optic design of head-up displays with freeform surfaces specified by NURBS’, Proc. SPIE 7100, 71000Y (2008).
- [8] <http://www.bmbf.de/de/16269.php>, 16.12.2011.
- [9] G. Davis, J. Roblee and A. Hedgesa, in ‘Comparison of freeform manufacturing techniques in the production’, Proc. SPIE 7426 742605-1 (2009).
- [10] S. Bäumer, in: ‘Handbook of Plastic optics’, 2nd edition (Wiley-VCH Verlag, Eindhoven, Netherlands, 2010) pp. 39–47, 56, 64, 199–201.
- [11] M. Hünten, F. Klocke, and O. Dambon. in ‘Precision glass molding: an integrative approach for the production of high precision micro-optics’, Proc. SPIE 7591, 75910X; doi:10.1117/12.840271 (2010).
- [12] M.P. Schaub, in ‘The Design of Plastic Optical Systems’ (SPIE Press, Bellingham, WA, 2009), pp. 47–55, 84.
- [13] R. Steinkopf, L. Dick, T. Kopf, A. Gebhardt, S. Risse, et al., in ‘Data handling and representation of freeform surfaces’, Proc. SPIE 81690X-9 (2011).
- [14] L. Piegl and W. Tiller, in ‘The NURBS Book’, 2nd edition (Springer Verlag, Tampa, Florida, 1997).
- [15] C. Brecher, M. Weck, M. Winterschladen, S. Lange, O. Wetter, et al., in ‘Manufacturing of free form surfaces in optical quality using an integrated NURBS data interface’, ASPE, Free-Form Optics: Design, Fabrication, Metrology, Assembly, 2004.
- [16] <http://industrial.panasonic.com>, Accessed 16 December, 2011.

- [17] L. Dick and R. Steinkopf, in 'Korrekturbearbeitung optischer Freiformflächen für sub- $\mu\text{m}$  – Formgenauigkeit im Spritzgusswerkzeug', *PHOTONIK*, 5/2010 (2010), pp. 44–46.
- [18] S. Scheiding et al., in 'References – a key issue for freeform structuring', *Structured and Freeform Surfaces Topical Meeting*, Euspen, Aachen, 10–11 February, 2010.
- [19] C. Buß and D. Lindemann, in 'Production of Freeform Optics', *EUSPEN Special Interest Group Meeting IPT Aachen*, 2010.
- [20] R. Steinkopf, A. Gebhardt, S. Scheiding, M. Rohde, O. Stenzel, et al., in 'Metal mirrors with excellent figure and roughness', *Proc. SPIE 7102, 71020C* (2008).
- [21] K. Rogers and J. Roblee, in 'Freeform Machining with Precitech Servo Tool Options', Available at: [www.ametek.com](http://www.ametek.com), downloaded 2010.
- [22] Y.-F. Dai, C. Guan, Z. -Q. Yin, G. -P. Tie, H. - F. Chen, et al., in 'Tool decentration effect in slow tool servo diamond turning off-axis conic aspheric surface', *5th International Symposium on Advanced Optical Manufacturing and Testing Technologies*, 2010.
- [23] M. Weinzierl, in 'Ultraprecision Machining in Optics Manufacturing', *Workshop/CAS Conference, Sinaia*, 2008.
- [24] T. Chang and E. Faison, *Polym. Eng. Sci.* 41, 703–710 (2001).
- [25] K. Mustafa, Y. Kaynak, O. S. Kamber, B. Mutlu, B. Bakir, et al., *Int. J. Adv. Manuf. Technol.* 46, 571–578 (2010).
- [26] C. H. Wu and Y.-J. Huang, *Int. J. Adv. Manuf. Technol.* 32, 1144–1154 (2007).
- [27] S. Stitz and W. Keller, in 'Spritzgießtechnik', 2 Auflage (Hanser Verlag, Würzburg, Germany, 2004), p. 108.
- [28] J. Zänkert, in 'Ergebnisbericht FINO (Flexible Prototypen- und reproduzierbare Serienfabrikation innovativer Optikelemente)', *Bundesministerium für Bildung und Forschung* (2006), pp. 33, 117.
- [29] L. Dick, in 'Freeform correction for molding high precision plane optical surfaces', *2nd EOS Conference on Manufacturing of Optical Components*, Munich, 2011.
- [30] O. Riemer, in 'Trennmechanismen und Oberflächenfeingestalt bei der Mikrozerspanung kristalliner und amorpher Werkstoffe', PhD thesis, University of Bremen, Shaker Verlag Aachen, 2001.



Lars Dick was born in Jena, Germany, on November 11, 1982. He studied Mechanical Engineering from 2002 to 2007 with a particular focus on Optics and Precision Engineering at the Technische Universität Ilmenau, where he graduated with a Diploma degree.

Since 2008 he is Head of the Ultra Precision Technology group at JENOPTIK Polymer

Systems GmbH. Also, since 2008, he is Research Associate at the Friedrich-Schiller-University in Jena, Germany. His research interests include diamond machining, replication techniques and metrology of optical surfaces.



Stefan Risse was born in Jena, Germany on April 27, 1964. He received a Diploma degree in Mechanical Engineering from the Technical College Zittau in 1990 and the Dr.-Ing. degree in Precision Engineering from the Technical University Ilmenau in 2001.

From 1990 to 1991 he worked at the Friedrich-Schiller-University in the field of Material Science. In 1992, he joined the Fraunhofer

Institute for Applied Optics and Precision Engineering IOF in Jena. Since 1995, he is the Head of the Precision Systems group at Fraunhofer IOF.



Andreas Tünnermann was born in Ahnsen, Germany on June 10, 1963. He received a Diploma and a PhD degree in Physics from the University of Hannover in 1988 and 1992, respectively. In 1997, he received an habilitation qualification.

He was head of the Department of Development at the Laser Zentrum Hannover from 1992 to 1997. In the beginning of 1998, he joined

the Friedrich-Schiller-University in Jena, Germany as a Professor and Director of the Institute of Applied Physics. In 2003, he additionally became the Director of the Fraunhofer Institute for Applied Optics and Precision Engineering IOF in Jena.

He is a sought-after expert in the Optics and Photonics Industry. He is founder and member of the Board of Directors of the industry driven cluster OptoNet Jena, one of the most dynamic regional optics clusters in Europe.

Andreas Tünnermann is a member of various societies, e.g., of the German Physical Society and the Optical Society of America. His research activities on Applied Quantum Electronics have been awarded, e.g., with the Gottfried-Wilhelm-Leibniz Award (2005).